International Refrigeration and Air Conditioning Conference

School of Mechanical Engineering

2016

Refrigerant Circuit Optimization of Dual-mode Single-Row Microchannel Heat Exchangers used for R410A Heat Pumps

Sunil Mehendale
Michigan Technological University, Houghton, MI, United States of America, ssmehend@mtu.edu

Zhenning Li
University of Maryland, College Park, MD, United States of America, znli@umd.edu

Vikrant Aute
University of Maryland, College Park, MD, United States of America, vikrant@umd.edu

Refrigerant Circuit Optimization of Dual-Mode Single-Row Microchannel Heat Exchangers used for R410A Heat Pumps

Sunil MEHENDALE[1]*, Zhenning LI[2], Vikrant AUTE [2]

[1]Michigan Technological University,
Houghton, MI, USA
Contact Information (ssmehend@mtu.edu)

[2]University of Maryland,
College Park, MD, USA
Contact Information (znli@umd.edu, vikrant@umd.edu)

* Corresponding Author

ABSTRACT

Microchannel heat exchangers (MCHX) are being increasingly applied in heat pumps because of their compactness, significant charge reduction, lower refrigerant pressure drop and lower air-side fan power consumption compared to traditional round tube-plate fin (RTPF) heat exchangers. Using a microchannel condenser as well as evaporator in a heat pump system also offers significant potential for cost reduction. Very few studies on pass optimization of microchannel condensers and evaporators have appeared in the literature, and even fewer exist on the circuit optimization of dual-mode MCHX used in a heat pump.

The influence of pass arrangement on the thermal-hydraulic performance of microchannel condensers and evaporators has been explored in this article. A total of 1982 configurations for 18 tube x 1.124 m, 36 tube x 0.562 m, and 54 tube x 0.375 m were simulated under conditions typically encountered by the outdoor unit of a R410A refrigerant-to-air heat pump. Two-, three-, and four-pass circuits with contracting, expanding, and equal pass designs were simulated using CoilDesigner. All designs had identical face area to allow a fair assessment of their performance.

For optimal condenser performance, 36 or 18 tube configurations are preferred to 54 tube designs. The 36 tube-31%/30%/25%/14%, 18 tube-56%/33%/11%, and 36 tube-25%/25%/25%/25% condenser coils have the best heat duty. Contracting or equal pass arrangements are superior to expanding pass arrangements for condensers.

Unlike condensers, 54 or 36 tube configurations yield the best evaporator heat duty. Again, quite contrary to condensers, expanding pass arrangements are clearly favored for optimal evaporator heat duty, and the best expanding pass arrangements significantly outperform the best contracting or equal pass arrangements. The 54 tube, 2%/4%/24%/70% and 2%/6%/93% evaporator coils are the best performing ones. Again, unlike in condensers, a strongly disproportionate distribution of tubes among the passes is favored for evaporators, with very few tubes recommended in the first pass or two, and many more tubes in the last pass. Additionally, evaporator performance is found to be much more sensitive to pass arrangement than condenser configurations. Hence, evaporator pass arrangements need more careful consideration than condenser pass arrangements.

Thus, quite contrary pass designs favor condenser and evaporator performance. This fact implies that to design dual-mode MCHX, as in a heat pump, some compromises will be necessary. Future work will address the performance of dual-mode MCHX at the component and system levels. The influence of air and refrigerant maldistribution on optimal MCHX pass arrangement will also be investigated.

1. INTRODUCTION

Microchannel heat exchangers (MCHX), both condensers (MCC) and evaporators (MCE), which were first applied in the automotive industry, have been, during the past 10-15 years, gradually adapted to residential and commercial HVAC&R products (Mehendale *et al.*, 2014). The traditional round tube-plate fin (RTPF) condenser is made of copper or aluminum tubes mechanically bonded to aluminum fins with heat transfer-enhancing features such as louvered fins. Unlike RTPF coils which are mechanically expanded, typically all-aluminum MCHX coils are brazed in a furnace. In the MCHX design, flat tubes having several small ports are used instead of round tubes. Figure 1 shows the general MCHX construction (2-pass shown for illustration) and Figure 2 depicts the principal geometric features of a typical tube and fin. In the current work, the thermal-hydraulic interaction between the air and refrigerant flows have been mathematically modeled for the configuration represented in Figure 1 and 2.

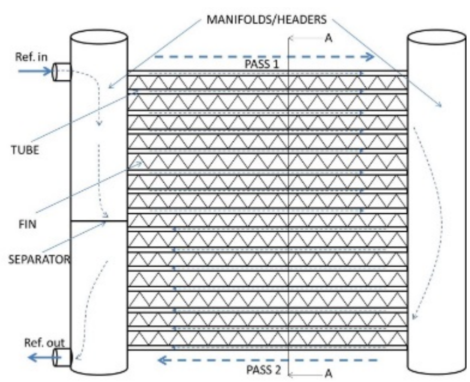

Figure 1: Basic MCHX building blocks

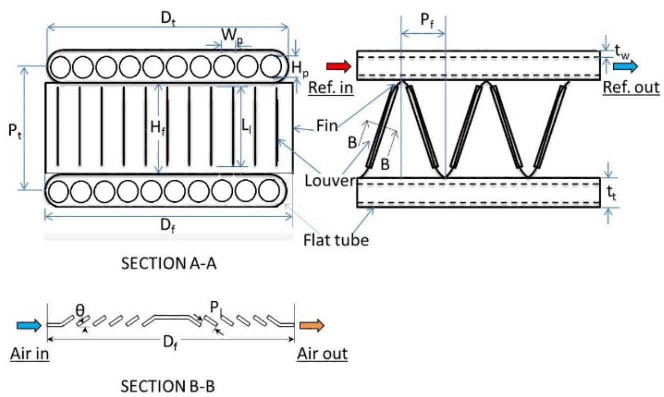

Figure 2: Key MCHX dimensions

As shown in Figure 1 and 2, a typical single row MCHX is made of four basic building blocks:
1. Flat microchannel tubes containing small ports (typically 1 mm or smaller in hydraulic diameter) through which refrigerant flows,
2. Corrugated louvered fins sandwiched between the microchannel tubes, through which air flows,
3. Two refrigerant manifolds for collecting and distributing refrigerant to or from the tubes, and
4. Pass separators for achieving the desired pass arrangement.

It is evident from Figures 1 and 2 that the air and refrigerant flow through the MCHX in a cross-flow arrangement. The four building blocks are joined using an aluminum-zinc alloy brazing material in a nitrogen-charged braze furnace to produce the completed MCHX. Different coil circuiting patterns or pass arrangements are accomplished by appropriately placing and brazing leak-free pass separator discs in the refrigerant manifolds to force the refrigerant to sequentially flow through selected groupings of flat tubes. The flat tubes allow the airside heat transfer surface area to be maximized, and the multiple tiny refrigerant channels within the flat tubes maximize the refrigerant side heat transfer by providing increased primary surface area and enhanced heat transfer coefficients. The metallurgical fin-tube bond resulting from the braze operation is designed to further enhance the heat transfer between the tubes and the fins. Due to a combination of all the above constructional features, the thermal performance of the MCHX is greatly enhanced. However, in order to achieve the best possible heat duty, it is of the utmost importance to select the best or optimum refrigerant circuiting or pass arrangement, and this choice rests entirely with the MCHX designer.

Compared to traditional RTPF heat exchangers, MCHX offer several benefits:
1. Improved or comparable heat transfer and about 65% lower refrigerant pressure drop. (Park and Hrnjak, 2008)
2. Up to about 10% lower refrigerant charge, due to the smaller internal volume of microchannel coils. (Park and Hrnjak, 2008)
3. Compact design, i.e., about two to three times higher surface area-to-volume ratio (Garimella, 2003), providing opportunities for weight, and hence, cost reduction.

Software capable of accurately capturing the complexities of two-phase flow and heat transfer in MCHX passages is a very appropriate tool for designing such products. Currently, several models for simulating MCHX performance are discussed in the literature. Such tools enable practitioners to cut down on the use of expensive tests. Here, a brief survey of MCHX simulation studies is presented, with a focus on pass arrangement analyses. Yin *et al.* (2001) developed a finite volume, first principles-based CO_2 gas cooler model. They employed empirical correlations to predict the heat transfer coefficients, pressure drop, and fin efficiency. Jiang *et al.* (2002) presented a simulation and optimization tool for designing air-to-refrigerant MCHX. An effectiveness-NTU method was employed to simulate dry surface conditions, while wet surface conditions were handled by the enthalpy potential method. The tool, CoilDesigner^{TM}, version 3.9.20141.203 (Jiang *et al.*, 2006), incorporates a network strategy for conveniently designing and analyzing coil circuiting. A segment-by-segment approach that accounts for two-dimensionally non-uniform air flow distribution across the coil face has been implemented within each tube. The model tracks and captures the significant change of thermophysical properties as the refrigerant undergoes phase transformation in the coil. It also provides a user-friendly graphical interface, and a choice of a wide variety of working fluids and air and liquid side heat transfer / pressure drop correlations.

Schwentker *et al.* (2005) verified the prediction of CoilDesigner^{TM} against experimentally measured data for eight R-134a microchannel condensers. The model was able to predict the condenser heat load within 2.25% for 80% of the 35 experimental data points. The average error, average absolute error, and the maximum error in the heat load prediction were -0.84%, 1.6%, and 4.6%, respectively.

In one of the most comprehensive microchannel condenser and gas cooler performance validation efforts, Huang *et al.* (2014) validated CoilDesigner^{TM} against 227 experimental data points for eight different working fluids including R410A and eighteen MCHX geometries from seven different data sources. The average absolute deviation between the predicted and measured values of the heat duty and the refrigerant pressure drop were found to be 2.7% and 28%, respectively.

More recently, Huang *et al.* (2015) validated the model against experimental data for condenser and evaporator applications using R410A and R32. 65 data points, including 45 condenser points and 20 evaporator points for eight different MCHX were validated. Without using any correction factors on the heat transfer correlations used in the model, the absolute average capacity prediction errors ranged from 1.75% to 3.1%, while the pressure drop deviations ranged from 11.14% to 16.71%.

Very few studies have aimed at understanding the principles behind optimizing refrigerant circuiting in single row MCHX. Huen and Dunn (1996 a) examined the effects of port diameter and shape on refrigerant circuit design in microchannel condensers. They conducted a single-phase heat exchanger analysis, which led them to conclude that smaller port sizes result in reduced heat exchanger internal volume and necessitate additional shorter parallel refrigerant passages. Port shape was shown to have a significant impact on heat exchanger volume and refrigerant circuiting. It was also demonstrated that the single-phase analysis was applicable to two-phase situations provided convective effects (e.g., annular flow condensation and convective boiling) were dominant. In a companion paper, Huen and Dunn (1996 b) investigated the effect of refrigerant pressure drop on microchannel condenser performance. They found that for a given port diameter, the pressure drop variation caused an optimal relationship between the number of parallel refrigerant passages and heat exchanger length. They concluded that an optimal combination of the number of ports and number of tubes minimized the condenser volume for a given port diameter.

Ye *et al.* (2009) analyzed a multiple parallel-pass (MPP) microchannel condenser for automotive air-conditioning systems. They introduced a flow distributor in the MPP condenser to enable parallel flow arrangement in adjacent flow paths. Through the MPP design, the two-phase zone was effectively enlarged to enhance the condensation heat transfer and reduce pressure drop. Performance test results showed that the heat duty of the MPP condenser was up to 9.5% higher than the traditional microchannel condenser.

Mehendale *et al.* (2014) employed CoilDesigner^{TM} to simulate a single row R410A-to-air microchannel condenser consisting of a fixed number of microchannel tubes and multi-louvered fins. The refrigerant mass flow rate through the condenser was fixed, while the outlet conditions were allowed to vary. The thermal-hydraulic performance of numerous two-, three-, and four-pass configurations was simulated over a range of tube lengths. Based on the tradeoffs encountered between condenser heat duty and refrigerant pressure drop, recommendations were provided to aid HVACR practitioners select the optimal pass arrangement for microchannel condensers similar to the one considered in that study. The analysis showed that for a 2.0 m long condenser, the 38%/31%/20%/11%, 42%/41%/17%, 23%/25%/25%/27%, 32%/34%/34%, 67%/33%, and 47%/53% configurations had the best heat transfer, in that order.

Recently, Mehendale *et al.* (2016) presented the results of the circuit optimization of a microchannel condenser used in an R600a (isobutane) heat pump. Two-, three-, and four-pass circuit arrangements in expanding, contracting, and equal configurations were explored. The number and length of MCHX tubes were varied so as to maintain a constant coil face area at a typical condenser operating condition in a residential heat pump. 36 tube x 0.562 m condenser coils were shown to provide the best heat duty among all possible contracting, expanding, and equal pass arrangements. The best contracting pass arrangement, 36%/36%/17%/11%, provided about 27% higher heat duty compared to 52%/48%, the worst.

It is thus clear that the principles governing the selection of the optimal pass or circuit arrangement for microchannel condensers or evaporators have not been explored in depth. Such studies on dual-mode heat exchangers, i.e., those used in heat pumps, are even scarcer. HVACR practitioners are commonly required to address and solve the question: for a given MCHX tube and louvered fin design (i.e., given building blocks), and pre-defined air velocity and refrigerant conditions at inlet and/or outlet of the heat exchanger, should a two-pass, a three-pass, or a four-pass circuit arrangement be preferred? Even if the number of passes can be determined from experience, how should the microchannel tubes be proportioned among the various passes? Normally, a costly and time-consuming heat exchanger and system-level test program coupled with simulation would be necessary to satisfactorily answer this question. In this article, the capabilities of CoilDesigner have been harnessed to shed light on this issue.

2. GEOMETRIC AND OPERATING CONDITIONS

In this section, the geometric and operating conditions used for the pass arrangement analysis are discussed. The MCHX tube and louvered fin geometry and the air and R410A side operating conditions selected for this study are summarized in Table 1. The coil face area for all configurations was fixed by decreasing the tube length while appropriately increasing the number of tubes. This allowed a fair comparison of the thermal-hydraulic performance of the various pass arrangements. R410A was chosen for the analysis because it is a very commonly used refrigerant in modern residential and commercial HVACR heat exchangers. The MCHX tube and fin dimensions are similar to heat exchangers typically applied in residential and commercial air-conditioning applications, and are identical to those used in Mehendale *et al.* (2016). However, unlike in Mehendale *et al.* (2014) where the R410A mass flow rate was held constant, here the evaporator outlet superheat and condenser outlet sub-cooling were fixed at 5°C, while the R410A mass flow rate was iteratively calculated to satisfy the air and R410A side operating conditions given in Table 2. This fact again ensures that all converged coil cases are compared on a fair basis. Table 3 lists the pressure drop and heat transfer correlations used in this analysis. It should be noticed that the operating conditions in Table 2 are representative of those an outdoor coil of a MCHX heat pump would experience in the summer and winter, respectively.

Table 1: MCHX tube and fin geometry used to analyze pass arrangements

Total number of tubes x Tube Length (m)	18 x 1.124	36 x 0.562	54 x 0.375
Tube depth, D_t (m)	0.0254		
Tube thickness, t_t (m)	0.0018		
Port diameter, D (m)	0.001		
Number of ports per tube	18		
Number of passes	2, 3, and 4		
Fin density, (fins per inch)	20		
Louver length, L_l (m)	0.0104		
Louver angle, θ (deg.)	30		
Louver pitch, P_l (m)	0.00152		
Fin height (m)	0.01641		

Table 2: Air and R410A operating conditions used in the analysis

Operating mode	Air inlet dry bulb (°C)	Air inlet wet bulb (°C)	Air face velocity (m/s)	R410A entering conditions	R410A leaving conditions
Condenser	35	23.9	2.0	45°C saturation temperature x 20°C superheat	5°C sub-cooling
Evaporator	8.33	6.11	2.0	45°C saturation temperature x 5°C subcooling (expansion valve inlet)	2°C saturation temp. x 5°C superheat

Table 3: Heat transfer and pressure drop correlations used in the analysis

	Air side	R410A side		
		Vapor	Two-Phase	Liquid
Heat transfer correlation	Chang and Wang (1997)	Dittus-Boelter (1985)	Shah (1979)	Dittus-Boelter (1985)
Pressure drop correlation	Chang *et al.* (2000)	Blasius (1996)	Chen *et al.* (2001)	Blasius, as quoted in Incropera and Dewitt (1996)

The following assumptions have been made in this investigation:

1. Air flow across the coil face is uniform. In practical applications, air flow non-uniformities arise from heat exchanger and fan configuration, duct design, and other similar factors which are beyond the scope of this work.
2. The distribution of refrigerant among the tubes of each pass, as well as the ports of each tube is uniform. However, it is recognized that refrigerant maldistribution might be important for certain MCHX design configurations.

Both these effects will be addressed in a future article.

3. RESULTS AND DISCUSSION

A large number of two-, three-, and four-pass configurations were analyzed in this work. For a given number of passes p in the MCHX, three basic types of pass configurations were investigated:

1. contracting,
2. expanding, and
3. equal pass arrangements.

Consider a coil with p passes and N[i] tubes in pass i, where i varies from 1 for the refrigerant inlet or first pass to p for the outlet or pth pass. A contracting pass arrangement is any pass arrangement that satisfies the following condition:

$$N[1] \geq N[2] \geq N[3] \dots\dots.. \geq N[p] \quad (1)$$

Similarly, an expanding pass arrangement is any pass arrangement that satisfies the requirement

$$N[1] \leq N[2] \leq N[3] \dots\dots.. N[p] \quad (2)$$

An equal pass arrangement is one where:

$$N[1] = N[2] = N[3] = \dots\dots\dots = N[p] \quad (3)$$

All possible contracting, expanding, and equal pass arrangements were automatically generated for the two-, three-, and four-pass arrangements using a self-developed code written for this purpose. 54 two-pass, 374 three-pass, and

1,554 four-pass combinations were simulated using the parametric pass arrangement analysis capability of CoilDesigner. It is worth remarking here that for microchannel condensers, a contracting pass arrangement is commonly considered to be preferable to an expanding one, and vice versa for microchannel evaporators. This is due to the fact that in condensers, the density of the refrigerant progressively increases as it flows through the condenser, thus necessitating successively smaller passes in the refrigerant flow direction, and vice versa for evaporators. Here, CoilDesigner has been efficiently used to explore numerous contracting, expanding, and equal pass arrangements, for condensers as well as evaporators, as discussed in sections 3.1 and 3.2.

3.1 Condenser Pass Optimization

Figure 3 shows the contracting and expanding / equal pass arrangements that yield the best heat duty for each combination of number of tubes and number of passes. There are nine such combinations: 18 tube-2 pass, 18 tube-3 pass, 18 tube-4 pass, 36 tube-2 pass, 36 tube-3 pass, 36 tube-4 pass, 54 tube-2 pass, 54 tube-3 pass, and 54 tube-4 pass. All bars (color-coded per the total number of tubes) in Figure 3 represent the heat duty of the best-performing tube-pass arrangement combination. The pass arrangement is shown in terms of the percentage of the total number of tubes on the abscissa. Thus, for instance, Figure 3 shows that the 36 tube-31%/31%/24%/14% condenser has the best heat duty (7.34 kW) not only among all possible 36 tube-4 pass arrangements, but also among all contracting pass arrangements simulated in this study.

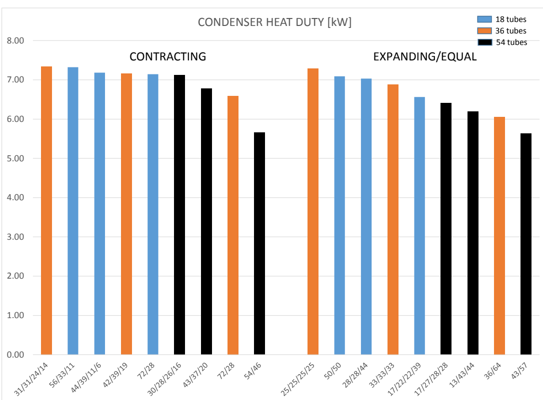

Figure 3: Best condenser pass arrangements

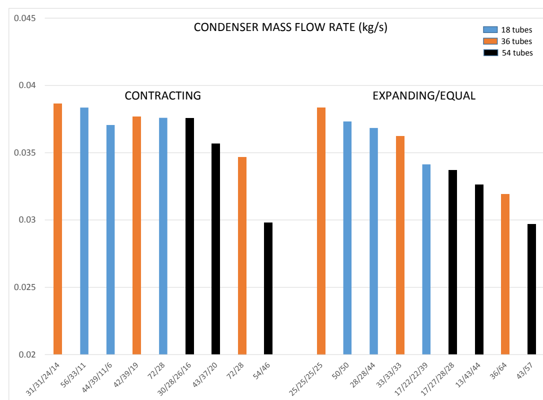

Figure 4: R410A mass flow rate through best condensers

The following important observations can be made by studying Figure 3.

a. Compared to 54 tube x 0.375 m configurations, it is clear that 36 tube x 0.562 m or 18 tube x 1.124 m condensers are preferred for optimizing their heat duty.
b. Among the contracting pass arrangements, the 36 tube, 31%/31%/24%/14% and the 18 tube, 56%/33%/11% condenser coils have the best heat duty. The 36 tube-4 equal pass arrangement coil has a heat duty comparable to these two configurations.
c. The top two pass arrangements among the expanding/equal options are both equal configurations. Thus, on the whole, compared to expanding pass arrangements, contracting or equal ones offer the best condenser heat duty.
d. The best contracting pass arrangement has about 23% higher heat duty compared to the worst contracting pass arrangement. Even for the 36 tube x 0.562 m configuration, the 42%/39%/19% design shows about 2.5% loss in heat duty compared to the 31%/31%/24%/14% configuration, which can be significant in an HVACR application. Thus, the importance of selecting the correct condenser coil configuration (number of tubes, length, and pass arrangement) cannot be overstated.

The relative performance of the top-performing pass arrangements shown in Figure 3 can be understood by plotting the refrigerant mass flow rate through them, as shown in Figure 4. It is seen that as the heat duty for either the contracting or the expanding/equal pass arrangements decreases (see Figure 3), on the whole, the R410A mass flow rate also decreases (see Figure 4). The heat duty and the R410A mass flow rate both drop by about 23% between the best and the worst-performing contracting as well as the equal/expanding pass arrangements. This trend is consistently true for the equal/expanding pass arrangements, while there is an exception among the contracting pass arrangements

– although the heat duty of the 36 tube, 42%/39%/19% design is 1.95% less than that of the 18 tube, 44%/39%/11%/6% configuration, its mass flow rate is actually higher by 1.65%. This behavior can be clarified by considering the refrigerant side conditions given in Table 2, under which the condenser operates. The R410A enthalpy at the entrance to all coils is fixed, because refrigerant enters all coils at a saturation temperature of 45°C and a superheat of 20°C. However, only the R410A outlet subcooling is specified to be 5°C. The outlet subcooled liquid enthalpy depends on the outlet temperature, which in turn, depends on the refrigerant mass flux, the pressure drop, the distribution of refrigerant phases in the coil, and therefore, the variation of the heat transfer coefficient in each pass.

Figure 5 shows the difference between the R410A inlet and exit enthalpy (Δh) across the condenser. As seen in Figure 5, the Δh for the 36 tube, 42%/39%/19% design is less than that of the 18 tube, 44%/39%/11%/6% configuration by about 1.95%. Since the heat duty is the product of the R410A mass flow rate and Δh, and, in this case, the latter dominates the former, it is reasonable that the 18 tube, 44%/39%/11%/6% configuration has better heat duty than the 36 tube, 42%/39%/19%.

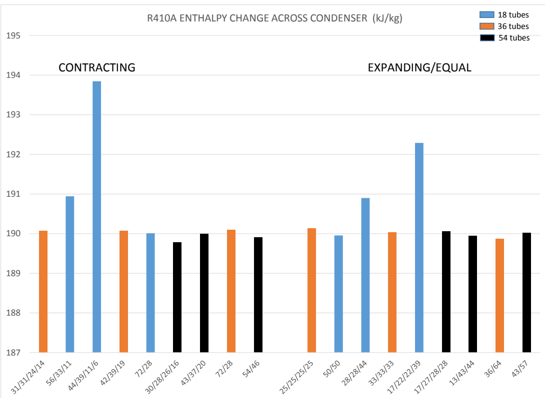

Figure 5: R410A enthalpy change across best condensers

3.2 Evaporator Pass Optimization

In this section, the key results of the evaporator pass optimization analysis are presented. Figure 6 shows the contracting and expanding / equal pass arrangements that yield the best evaporator heat duty for each combination of number of tubes and number of passes.

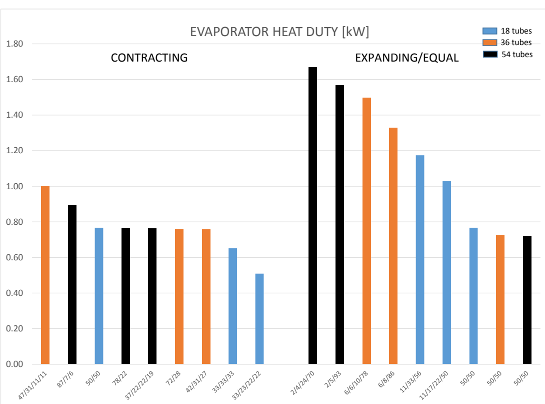

Figure 6: Best evaporator pass arrangements

Careful study of Figure 6 leads to the following key findings:

a. Compared to 18 tube x 1.124 m configurations, 54 tube x 0.375 m or 36 tube x 0.562 m evaporators are preferred for optimizing their heat duty.
b. Unlike in condensers, there is a clear preference for expanding pass arrangements to optimize the evaporator heat duty. The best expanding pass arrangements significantly outperform the best contracting or equal pass

arrangements.

c. Among the expanding pass arrangements, the 54 tube, 2%/4%/24%/70% and 2%/5%/93% evaporator coils are the best performing. Thus, a strongly asymmetric distribution of tubes among the passes, with very few tubes in the first pass or two, and many tubes in the last pass is the preferred configuration for evaporators.

d. The best expanding pass arrangement has about 131% higher heat duty compared to the worst expanding pass arrangement. Even for the 54 tube x 0.375 m configuration, the 2%/5%/93% design shows about 6% loss in heat duty compared to the 2%/4%/24%/70% configuration, which can be quite significant in an HVACR application. This finding shows that evaporator pass arrangements are more sensitive than condenser configurations in terms of optimizing their heat duty. Thus, it becomes even more important to design the correct evaporator coil configuration (number of tubes, length, and pass arrangement) compared to condensers.

The relative performance of the best evaporator pass arrangements shown in Figure 6 can be understood by plotting the refrigerant mass flow rate through them, as shown in Figure 7. It is seen that as the heat duty for either the contracting or the expanding/equal pass evaporators decreases (see Figure 6), on the whole, the R410A mass flow rate also decreases (see Figure 7). However, there are exceptions to this trend among the contracting as well as the expanding / equal evaporator pass arrangements – for example, although the heat duty of the 18 tube, 11%/33%/56% design is 11.6% less than that of the 36 tube, 6%/8%/86% configuration, its mass flow rate is actually higher by 6.7%. It is such exceptions that require a more detailed analysis and explanation. This behavior can be clarified by considering the refrigerant side conditions given in Table 2, under which the evaporator operates. The R410A enthalpy at the exit of all coils is fixed, because refrigerant leaves all coils at a saturation temperature of 2°C and a superheat of 5°C. However, since the refrigerant enters the expansion device at 45°C saturation temperature and 5°C subcooling, only the R410A enthalpy entering the evaporator is fixed. The R410A saturation temperature, pressure, and enthalpy entering the evaporator in each case are determined by the distribution of the refrigerant mass flux, the pressure drop, the distribution of refrigerant phases, and therefore, the variation of the heat transfer coefficient among the various passes. For the case under consideration, as seen in Figure 8, the 18 tube, 11%/33%/56% has 17.2% lower enthalpy increase across the evaporator compared to the 36 tube, 6%/8%/86% design. Since the drop in enthalpy increase across the evaporator dominates the increase in refrigerant mass flow rate, the heat duty of the 18 tube, 11%/33%/56% design is actually lower than that of the 36 tube, 6%/8%/86% design by 11.6%.

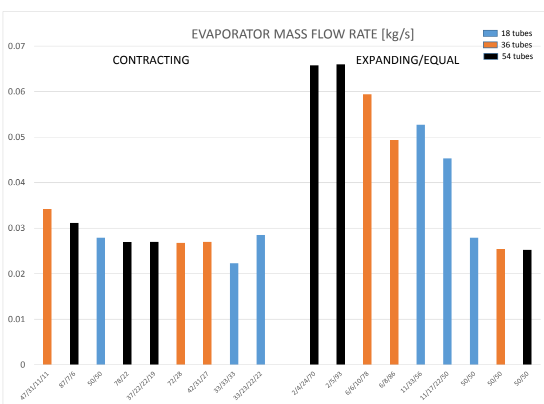

Figure 7: R410A mass flow rate for best evaporators

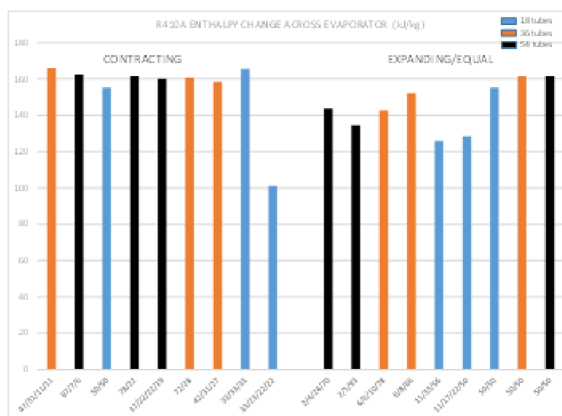

Figure 8: R410A enthalpy change across best evaporators

4. CONCLUSIONS AND FUTURE WORK

The influence of pass arrangement on the thermal-hydraulic performance of dual-mode microchannel condensers and evaporators has been explored in this article. 1982 coils comprising 18 tube x 1.124 m, 36 tube x 0.562 m, and 54 tube x 0.375 m embodiments were simulated under conditions typical of those encountered by the outdoor unit of a R410A refrigerant-to-air heat pump. Two-, three-, and four-pass circuits with contracting, expanding, and equal pass designs were investigated using CoilDesigner. All designs had identical face area to allow a fair assessment of their performance.

For optimal condenser performance, 36 tube x 0.562 m or 18 tube x 1.124 m configurations are preferred to 54 tube x 0.375 m designs. The 36 tube, 31%/31%/24%/14%, the 18 tube, 56%/33%/11%, and the 36 tube-4 equal pass arrangement condenser coils have the best heat duty. On the whole, contracting or equal pass arrangements offer the best condenser heat duty compared to expanding pass arrangements.

The best contracting pass arrangement has about 23% higher heat duty compared to the worst contracting pass arrangement. Even for the 36 tube x 0.562 m configuration, the 42%/39%/19% design shows about 2.5% loss in heat duty compared to the 31%/31%/24%/14% configuration, which can be significant in an HVACR application. This finding emphasizes the importance of appropriately selecting the condenser coil configuration (number of tubes, length, and pass arrangement).

Compared to 18 tube x 1.124 m designs, 54 tube x 0.375 m or 36 tube x 0.562 m configurations yield the best evaporator heat duty. Quite unlike condensers, expanding pass arrangements are clearly favored for optimal evaporator heat duty. The analysis shows that the best expanding pass arrangements significantly outperform the best contracting or equal pass arrangements. The 54 tube, 2%/4%/24%/70% and 2%/5%/93% evaporator coils are the best performing ones. Again, unlike in condensers, a strongly disproportionate distribution of tubes among the passes is favored for evaporators, with very few tubes in the first pass or two, and many more tubes in the last pass. The second-best evaporator design, the 54 tube x 0.375 m, 2%/5%/93% configuration shows about 6% loss in heat duty compared to the best 2%/4%/24%/70% configuration, which can be quite significant in an HVACR application. Thus, evaporator performance is much more sensitive to pass arrangement than condenser configurations. Therefore, designing evaporator pass arrangements demands a more careful understanding of the principles and tradeoffs involved in selecting non-optimal configurations.

This study reveals that quite contrary factors favor the optimal performance of condensers and evaporators. This fact implies that if the same MCHX configuration is to serve as a condenser in the summer, and an evaporator in the winter, as in the outdoor unit of a heat pump, some design compromises will be necessary. In future development of this work, we plan to address the performance of dual-mode MCHX, also taking their system-level performance into consideration. The influence of air flow and refrigerant maldistribution on optimal MCHX pass arrangement will also be investigated.

NOMENCLATURE

D_f	fin depth	(m)
D_t	tube depth	(m)
Δh	refrigerant enthalpy change across heat exchanger	(kJ/kg)
H_f	fin height	(m)
i	pass number beginning with inlet pass	(-)
L_l	louver length	(m)
MCC	microchannel condenser	
MCE	microchannel evaporator	
MCHX	microchannel heat exchanger	
N[i]	number of tubes in pass i	(-)
p	maximum number of passes	(-)
P_f	fin pitch	(m)
P_l	louver pitch	(m)
P_t	tube pitch	(m)
t_t	tube thickness	(m)
t_w	tube wall thickness	(m)
θ	louver angle	(deg.)

REFERENCES

Chang, Y., Chang, H., Tsai, L., Wang, C. (2000). A Generalized Friction Correlation for Louver Fin Geometry. *Int. J. Heat Mass Tran*, 43(12), 2237-2243.

Chang, Y., Wang, C. (1997). A Generalized Heat Transfer Correlation for Louver Fin Geometry. *Int. J. Heat Mass Tran.*, 40(3), 533-544.
Chen, I. Y., Yang k.-S., Chang, Y., Wang, C. (2001). Two-Phase pressure drop of air-water and R-410A in small horizontal tubes. *Int. J. Multiphase flow*, 27, 1293-1299
Dittus, F. W., Boelter, L.M.K. (1985), Heat Transfer in Automobile Radiators of the Tubular Type. *Int. Comm. Heat and Mass Transfer*, 12(1), 3-22.
Garimella, S. (2003), Innovations in Energy Efficient and Environmentally Friendly Space-Conditioning Systems, *Energy*, 28, 1593–1614.
Huang, L., Aute, V., Radermacher, R. (2014). A Model for Air-To-Refrigerant Microchannel Condensers with Variable Tube and Fin Geometries. *Int. J. Refrig*., 40, 269-281.
Huang, L., Bacellar, D., Aute, V., Radermacher, R. (2015). Variable geometry microchannel heat exchanger modeling under dry, wet, and partially wet surface conditions accounting for tube-to-tube heat conduction. *Science and Technology for the Built Environment*, 21(5): p. 703-717.
Huen, M., Dunn, W. (1996 a). Principles of Refrigerant Circuiting with Application to Microchannel Condensers: Part I - Problem Formulation and the Effects of Port Diameter and Port Shape, *ASHRAE Trans.*, *ASHRAE, Atlanta, GA*, 102, 373-381.
Huen, M., Dunn, W. (1996 b), Principles of Refrigerant Circuiting with Application to Microchannel Condensers: Part II - The Pressure-Drop Effect and the Cross-Flow Heat Exchanger Effect, *ASHRAE Trans*., ASHRAE, Atlanta, GA, 102, 382-383.
Incropera F.P. and DeWitt D. P. (1996). *Introduction to heat transfer*. (3rd ed.), New York, NY: John Wiley & Sons.
Jiang, H., Aute, V., Radermacher, R., 2002, A User-Friendly Simulation and Optimization Tool for Design of Coils, *Proc. 9th Int. Refrig. Air Cond. Conf. at Purdue*, Purdue University, West Lafayette, IN, Paper R5-1.
Jiang H., Aute V., Radermacher R. (2006). CoilDesigner: A General Purpose Simulation and Design Tool for Air to Refrigerant Heat Exchangers, *Int. J. Refrig.*, 29,(4), 601-610.
Mehendale, S., V. Aute, and R. Radermacher. (2014). Principles of Refrigerant Circuit Optimization in Single Row Microchannel Condensers. *Int. Refrigeration and Air Conditioning Conference, Purdue University, West Lafayette, IN, USA.*
Mehendale, S., V. Aute, and R. Radermacher. (2016). Optimization of Pass Arrangements for Microchannel Heat Pump Condensers Using Isobutane. *12th IIR Gustav Lorentzen Natural Working Fluids Conference, Edinburgh*
Park, C., Hrnjak, P. (2008). Experimental and Numerical Study on Microchannel and Round-Tube Condensers in a R410A Residential Air-Conditioning System, *Int. J. Refrig.*, 31, 822-831.
Schwentker, R.A., Aute, V.C., Radermacher, R., Mercer, K.B. (2005). Simulation and Design Tool for Microchannel Heat Exchangers, *Proc. Fifth Int. Conf. Enhanced, Compact, and Ultra-Compact Heat Exchangers: Science and Technology*, Eds. R.K. Shah, M. Ishizuka, T.M. Rudy, and V.V. Wadekar, Hoboken, NJ, USA., Paper CHE 2005-24.
Shah, M. (1979). A General Correlation for Heat Transfer during Film Condensation inside Pipes, *Int. J. Heat Mass Tran.*, 22, 547-556.
Ye, L., Tong, M., Zeng, X. (2009). Design and analysis of multiple parallel-pass condensers, *Int. J. Refrig.*, 32, 1153-1161.
Yin, J., Bullard, C., Hrnjak, P. (2001). R-744 Gas Cooler Model Development and Validation, *Int. J. Refrig.*, 24, 692-701.